

DFPD 00/TH/08
UNICAL-TH 00/1
BITP-00-05E
February 2000

THE POMERON AS A FINITE SUM OF GLUON LADDERS \diamond

R. Fiore^{a†}, L.L. Jenkovszky^{b§}, A. Lengyel^{c§}, F. Paccanoni^{d*}, A. Papa^{a†}

^a *Dipartimento di Fisica, Università della Calabria,
Istituto Nazionale di Fisica Nucleare, Gruppo collegato di Cosenza
I-87036 Arcavacata di Rende, Cosenza, Italy*

^b *Bogoliubov Institute for Theoretical Physics,
Academy of Sciences of the Ukraine
252143 Kiev, Ukraine*

^c *Institute of Electron Physics,
v. Universitetska 21, 88000 Uzhgorod, Ukraine*

^d *Dipartimento di Fisica, Università di Padova,
Istituto Nazionale di Fisica Nucleare, Sezione di Padova
via F. Marzolo 8, I-35131 Padova, Italy*

Abstract

A model for the Pomeron at $t = 0$ is suggested. It is based on the idea of a finite sum of ladder diagrams in QCD. Accordingly, the number of s -channel gluon rungs and correspondingly the powers of logarithms in the forward scattering amplitude depends on the phase space (energy) available, i.e. as energy increases, progressively new prongs with additional gluon rungs in the s -channel open. Explicit expressions for the total cross section involving two and three rungs or, alternatively, three and four prongs (with $\ln^2(s)$ and $\ln^3(s)$ as highest terms) is fitted to the proton-proton and proton-antiproton total cross section data in the accelerator region.

PACS numbers: 11.80.Fv, 12.40.Ss, 13.85.Kf.

** Work supported by the Ministero italiano dell'Università e della Ricerca Scientifica e Tecnologica and by the INTAS.*

[†]*e-mail address:* FIORE, PAPA@CS.INFN.IT

[‡]*e-mail address:* JENK@BITP.KIEV.UA

[§]*e-mail address:* SASHA@LEN.UZHGOROD.UA

^{*}*e-mail address:* PACCANONI@PD.INFN.IT

1 Introduction

It is widely accepted that the Pomeron in QCD corresponds to an infinite gluon ladder with Reggeized gluons on the vertical lines (see Fig. 1), resulting [1, 2, 3] in the so-called supercritical behavior $\sigma_t \sim s^{\alpha(0)}$, where $\alpha(0)$ is the intercept of the Pomeron trajectory. However, at finite energies only a finite number of diagrams contributes. The lowest order diagram is that of two-gluon exchange, first considered by Low and Nussinov [4]. The next order, involving an s -channel gluon rung, was studied e.g. in the papers [2, 5]. The problem of calculating these diagrams is twofold. One problem is connected with the non-perturbative contributions to the scattering amplitude in the “soft” region. It may be ignored by “freezing” the running coupling constant at some fixed value of the momentum transfer and assuming that the forward amplitude can be cast by a smooth interpolation to $t = 0$. More consistently, one introduces a non-perturbative model [6] of the gluon propagator valid also in the forward direction. The second problem is more technical: at any given perturbative order α_s^n , the leading contribution in the $s \rightarrow \infty$ limit, proportional to $(\alpha_s \ln(s))^n$, is given by a subset of all the Feynman diagrams contributing at that perturbative order; each of these diagrams consists of a leading term in the $s \rightarrow \infty$ limit and of a non-leading, negligible part. The leading contributions from all orders in perturbation theory can be resummed [1, 2, 3]. For non-asymptotic energies, however, at any order in the coupling constant subleading terms are present coming both from the neglected diagrams and from the neglected part of the leading diagrams. Although functionally the result is always the sum of increasing powers of logarithms, the numerical values of the coefficients entering the sum is lost unless all diagrams are calculated.

The summation and convergence of an infinite series is a known problem in physics. As discussed in a recent paper [7], various situations may occur, where a

finite series approximates the exact result better than the infinite sum does. Since, as stressed above, the coefficients of the perturbative series are not known from QCD even for $t = 0$ (their calculation in the non-forward direction is much more tricky), the convergence of the series is also unknown.

Conversely, one can expand the "supercritical" Pomeron $\sim s^{\alpha(0)}$ in powers of $\ln(s)$. Such an expansion is legitimate within the range of active accelerators, i.e. near and below the TeV energy region, where fits to total cross sections by a power or logarithms are known [8] to be equivalent numerically. Moreover, forward scattering data (total cross sections and the ratio of the real to the imaginary part of the forward scattering amplitude) do not discriminate even between a single and quadratic fit in $\ln(s)$ to the data.

Phenomenologically, more information on the nature of the series can be gained if the t dependence is also involved. The well-known (diffractive) dip-bump structure of the differential cross section can be roughly imitated by the Glauber (or eikonal) series, although more refined studies within the dipole Pomeron model (DP) (linear behavior in $\ln(s)$) [9] show that the relevant series is not just the Glauber (eikonal) one. A generalization of the DP model including higher terms in $\ln(s)$ was considered in [10]. We mention these attempts only for the sake of completeness, although we stick to the simplest case of $t = 0$, where there are hopes to have some connection with the QCD calculations.

In the present paper we consider a new parametrization for total cross sections based on the contribution of a finite series of QCD diagrams with relative weights (coefficients) and rapidity gaps to be determined from the data. Each set of the diagrams is "active" in "its zone", i.e. the parameters should be fitted in each energy

interval separately and the relevant solutions should match. The matching procedure will be similar to that known for the wave functions in quantum mechanics, i.e. we require continuity of the total cross section and of its first derivative.

2 Description of the model and an example with two gluon rungs

The Pomeron contribution to the total cross section is represented in the form

$$\sigma^P(s) = \sum_{i=0}^N f_i(s) \theta(s - s_0^i) \theta(s_0^{i+1} - s) , \quad (1)$$

where

$$f_i(s) = \sum_{j=0}^i a_{ij} L^j , \quad (2)$$

s_0 is the prong threshold, $\theta(x)$ is the step function and $L \equiv \ln(s)$. Here and in the following, for s and s_0 it is understood $s/(1 \text{ GeV}^2)$ and $s_0/(1 \text{ GeV}^2)$, respectively. The main assumption in Eq. (1) is that the widths of the rapidity gaps $\ln(s_0)$ are the same along the ladder and are energy independent. Their magnitude is not known *a priori*, but can be related to correlations between jets or multiclusters [11] formed by single gluons or determined empirically. The functions $f_i(s)$ are finite polynomials in L , corresponding to finite gluon ladder diagrams in QCD, where each power of the logarithm collects all the relevant diagrams. Each time the rapidity gap $\sim \ln(s)$ exceeds the threshold value $\ln(s_0)$, a new prong opens adding a new power in L .

In Eq. (1) the sum over N is a finite one, since N is proportional to $\ln(s)$, where s is the present squared c.m. energy. Hence this model is quite different

from the usual approach where, in the limit $s \rightarrow \infty$, the infinite sum of the leading logarithmic contributions gives rise to an integral equation for the amplitude.

To make the idea more clear, we first describe the mechanism in the case of three gaps (two rungs) with

$$f_0(s) = a_{00} , \quad (3)$$

$$f_1(s) = a_{10} + a_{11}L , \quad (4)$$

$$f_2(s) = a_{20} + a_{21}L + a_{22}L^2 . \quad (5)$$

By imposing the requirement of continuity (of the cross section and of its first derivative) one constrains the parameters. E.g., from the equality $f_1(s_0) = f_0(s_0)$ the relation

$$a_{10} = a_{00} - a_{11} \ln(s_0) \quad (6)$$

follows. Furthermore, from $f_2(s_0^2) = f_1(s_0^2)$ one gets

$$a_{20} = -2a_{21} \ln(s_0) - 4a_{22} \ln^2(s_0) + a_{10} + 2a_{11} \ln(s_0) \quad (7)$$

and from the continuity of the relevant derivatives

$$a_{21} = a_{11} - 4a_{22} \ln(s_0) \quad (8)$$

follows.

To remedy the effect of the opening prongs and get a smooth behavior at low energies, we have included also a Pomeron daughter, behaving like $\sim 1/s$, to the Eqs. (3) and (4) with parameters b_0 and b_1 respectively (otherwise the continuity condition could not be applied to the first, constant term, whose derivative vanishes).

In fitting the model to the data, we rely mainly on $\bar{p}p$ data that extend to the highest (accelerator) energies, to which the Pomeron is particularly sensitive. To increase the confidence level, pp data were included in the fit as well. To keep the number of free parameters as small as possible and following the successful phenomenological approach of Donnachie and Landshoff [12], a single “effective” Reggeon trajectory with intercept $\alpha(0)$ will account for non-leading contributions, thus leading to the following form for the total cross section:

$$\sigma_t(s) = \sigma^P(s) + R(s) , \quad (9)$$

where $\sigma^P(s)$ is given by Eq. (1) and $R(s) = as^{\alpha(0)-1}$ (the parameter a is different for $\bar{p}p$ and pp and is considered as an additional free parameter).

Ideally, one would let free the width of the gap s_0 and consequently the number of gluon rungs (highest power of L). Although possible, technically this is very difficult. Therefore we proceed by trial and error, i.e. make fits for fixed (two and three) number of rungs (power of the logarithms). Even within this approximation there is some room, as we shall see, to study the s_0 dependence of the results.

Notice that the values of the parameters depend on the energy range of the fitting procedure. For example, the values of the parameters in f_0 if fitted in “its” range, i.e. for $s \leq s_0$, will get modified with the higher energy data and correspondingly higher order diagrams included.

Fits to the $\bar{p}p$ and pp data were performed from $\sqrt{s} = 4$ up to the highest energy Tevatron data (for $\bar{p}p$), including all the results from there [14]. To cover the energy range with equal rapidity gaps uniformly, s_0 was chosen to be equal to 144.

The resulting fit is shown in Fig. 2. The values of the fitted parameters are

quoted in Table 1.

3 Three gluon rungs and fits to the $p\bar{p}$ and pp data

We cover the energy span available in the accelerator region by four gaps resulting in three gluon rungs and consequently L^3 as the maximal power. The individual Pomeron terms and relevant gaps now are

$$4 \geq \sqrt{s} \leq \sqrt{s_0} \quad : \quad f_0 = a_{00} + b_0/s , \quad (10)$$

$$\sqrt{s_0} \geq \sqrt{s} \leq (\sqrt{s_0})^2 \quad : \quad f_1 = a_{10} + b_1/s + a_{11}L , \quad (11)$$

$$(\sqrt{s_0})^2 \geq \sqrt{s} \leq (\sqrt{s_0})^3 \quad : \quad f_2 = a_{20} + a_{21}L + a_{22}L^2 , \quad (12)$$

$$(\sqrt{s_0})^3 \geq \sqrt{s} \leq (\sqrt{s_0})^4 \quad : \quad f_3 = a_{30} + a_{31}L + a_{32}L^2 + a_{33}L^3 . \quad (13)$$

As in the case of three gaps, the individual Pomeron terms and their derivatives were matched at the prong values. E.g. a_{10} was determined from the condition $f_0(s_0) = f_1(s_0)$, while from the equality of the relevant derivatives, b_1 can be expressed in terms of the other parameters. Ultimately, we are left with nine free parameters: a_{00} , b_0 , a_{11} , a_{22} , a_{32} and a_{33} , each determined in its range, while a and $\alpha(0)$ are fitted in the whole range of the data. The parameter s_0 in principle is also free, but as discussed above, we determine it by trial and error, starting with the value $s_0 = 64$. The gap width was chosen such as to cover the whole rapidity span by at most four gaps (to have L^3). The final value for s_0 turned out to be 42.5, resulting in a sequence of energy intervals ending at $\sqrt{s} = 1800$.

Fig. 3 shows our fit to the $p\bar{p}$ and pp total cross section data. The values of the fitted parameters are quoted in Table 2. The value of the $\chi^2/\text{d.o.f.}$ is ~ 1.3 , much

better than in the case of two gluon rungs.

The value of the effective Reggeon intercept remains rather low, close to 0.5 (compare for example with Ref. [13]), however interestingly enough its value is correlated with the gap width: the smaller the gap width, the higher the Reggeon intercept.

4 Conclusions

Although high quality fits were not the primary goal of the present study, we may conclude that our results are comparable with those of similar analyses [12]. There is still room for some technical improvements in this direction. Our main goal instead was to seek for a correct form of the “perturbative” series of total cross sections and for regularities in the behavior of the parameters. In fact we find that the coefficients in front of leading logarithms in the Pomeron contribution are related roughly by a factor 1/10. Notice the alternating signs in front of the logarithms. They may reflect the fact discussed in the introduction, namely that each power of the logarithms collects various contributions of the same order but from different diagrams (see Fig. 1).

“Footprints” of the prongs at low energies are slightly visible in Fig. 2 (especially in the case of pp scattering where the contribution from secondary Reggeons is smaller than in $\bar{p}p$). A more detailed study of this phenomenon could answer the question whether this is an artifact or a manifestation of the Pomeron’s basic properties.

The present model and its experimental verification may shed light also on the

energy range of the applicability of various approximations to the Pomeron. The simplest, Low-Nussinov model with constant cross sections is a crude approximation to reality. The inclusion of one gluon rung may be associated with the dipole Pomeron. This model has many attractive features, such as selfconsistency with respect to s -channel unitarity. Note that $\ln(s)$ is the strongest rise within the Regge pole model. The next order, $\ln^2(s)$, conflicts with the unitarity bound, requiring that the rise of the cross section does not exceed that of the slope parameter (shrinkage of the cone), that in the Regge approach is at most $\ln(s)$ (unless special assumptions are involved) . This regime seems typical of the Tevatron energy region. The role and weight of higher order terms is interesting, but needs more care for two reasons: first, too many free parameters make their determination difficult and secondly, they violate the Froissart bound, therefore eikonal corrections - otherwise present everywhere - here become crucial. A generalization of the above procedure within the eikonal model is possible, although the calculations (matching, fitting) become more complicated.

Extrapolations to still higher energies are of great interest. By fitting the model to the cosmic ray data and/or future (RHIC, LHC) accelerator data, one could explore the role of the new thresholds. On the other hand, from the present fits and, hopefully, from the QCD calculations one may try to deduce recursion relations and try to extrapolate the value of the coefficients in front of the logarithms. In any case, the higher the energy, the more important the unitarity corrections will become. Future fits of the model to various data may settle some details left open by this paper.

5 Acknowledgment

We thank V.S. Fadin, E.A. Kuraev and L.N. Lipatov for numerous discussions on the BFKL Pomeron.

References

- [1] E.A. Kuraev, L.N. Lipatov, V.S. Fadin, Zh. Eksp. Teor. Fiz. **72**, 377 (1977) [Sov. Phys. JETP **45**, 199 (1977)].
- [2] Y.Y. Balitzkij, L.N. Lipatov, Sov. J. Nucl. Phys. **28**, 822 (1978).
- [3] L.N. Lipatov, Zh. Eksp. Teor. Fiz. **90**, 1536 (1986) [Sov. Phys. JETP **63**, 904 (1986)];
- [4] F.E. Low, Phys. Rev. **D12** (1975) 163;
S. Nussinov, Phys. Rev. Lett. **35**, 1286 (1975).
- [5] B.M. McCoy, T.T. Wu, Phys. Rev. **D12**, 3257 (1975);
L.L. Frankfurt, V.E. Sherman, Sov. J. Nucl. Phys. **23**, 581 (1976);
L. Tybursky, Phys. Rev. **D13**, 1107 (1976).
- [6] P.V. Landshoff, O. Nachtmann, Z. Phys. **C35**, 405 (1987);
F. Halzen, G. Krein, A.A. Natale, Phys. Rev. **D47**, 2324 (1994);
L.L. Jenkovszky, A. Kotikov, F. Paccanoni, Z. Phys. **C63**, 131 (1994).
- [7] G.B. West, *Asymptotic Series and Precocious Scaling*, hep-ph/0011416.
- [8] J.R. Cudell, V. Ezhela, K. Kang, S. Lugovsky, N. Tkachenko, *High-Energy Forward Scattering and the Pomeron: Simple Pole versus Unitarized Models*, BROWN-HET-1184, IHEP 99-32, KIAS-P99070, ULG-PNT-99-JRC-1, hep-ph/9908218.
- [9] L.L. Jenkovszky, A.N. Shelkovenko, B.V. Struminsky, Z. Phys. **C36**, 17 (1987).
- [10] P. Desgrolard, M. Giffon, L.L. Jenkovszky, Yad. Fiz. **56-10**, 226 (1993) [Phys. Atom. Nucl. **56-10**, 1429 (1993)].
- [11] A. Bassetto, F. Paccanoni, Nuovo Cim. **2A**, 306 (1971).

- [12] A. Donnachie and P.V. Landshoff, Phys. Lett. **B123**, 345 (1983); Nucl. Phys. **B266**, 690 (1986).
- [13] A. Capella, A. Kaidalov, C. Merino, J. Tran Thanh Van, Phys. Lett. **B337**, 358 (1994).
- [14] F. Abe et al. (CDF Collaboration), Phys. Rev. **D50**, 5550 (1994); N. Amos et al., Nucl. Phys. **B262**, 689 (1985);
K.J. Foley et al., Phys. Rev. Lett. **19**, 857 (1967);
S.P. Denisov et al., Phys. Lett. **B36**, 415 (1971);
A.S. Carroll et al., Phys. Lett. **B61**, 303 (1976), *ibidem* **B80**, 423 (1979);
M. Honda et al., Phys. Rev. Lett. **70**, 525 (1993).

TABLES

s_0	b_0	b_1	$\alpha(0)$	$a_{p\bar{p}}$	a_{pp}
144	-74.4	421	0.421	127	45.9
a_{00}	a_{10}	a_{11}	a_{20}	a_{21}	a_{22}
35.7	15.2	3.44	57.3	-5.03	0.427

Table 1: Fitted parameters in the case of two rungs. The parameters b_i and $a_{...}$ are given in units of 1 mb.

s_0	b_0	b_1	$\alpha(0)$	$a_{p\bar{p}}$	a_{pp}
42.5	-89.3	43.0	0.550	105	56.3
a_{00}	a_{10}	a_{11}	a_{20}	a_{21}	a_{22}
30.6	15.5	3.22	27.3	0.0629	0.211
a_{30}	a_{31}	a_{32}	a_{33}		
106.	-18.7	1.68	-0.0376		

Table 2: Fitted parameters in the case of three rungs. The parameters b_i and $a_{...}$ are given in units of 1 mb. The value of the $\chi^2/\text{d.o.f.}$ is ~ 1.3 .

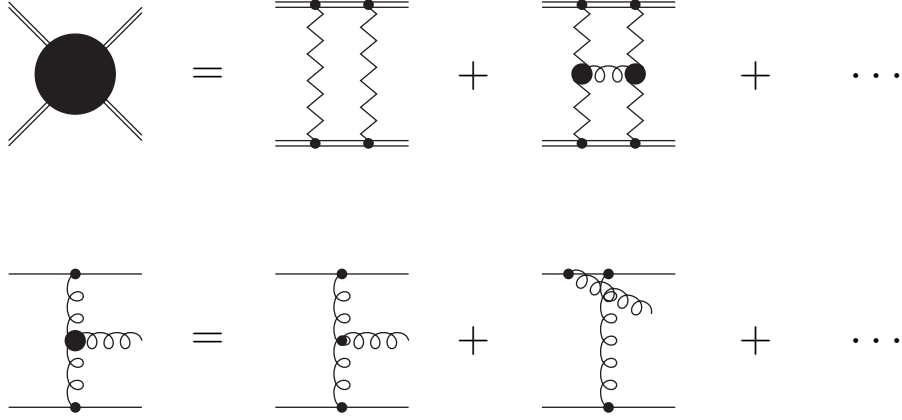


Figure 1: Schematic representation of the total cross section in the leading $\ln(s)$ approximation (first row). Double lines represent protons or anti-protons, vertical zig-zag lines are Reggeized gluons, horizontal wavy lines are gluons. The effective vertex for two Reggeized gluons and one gluon is defined in the second row. Here external lines can represent quarks or gluons.

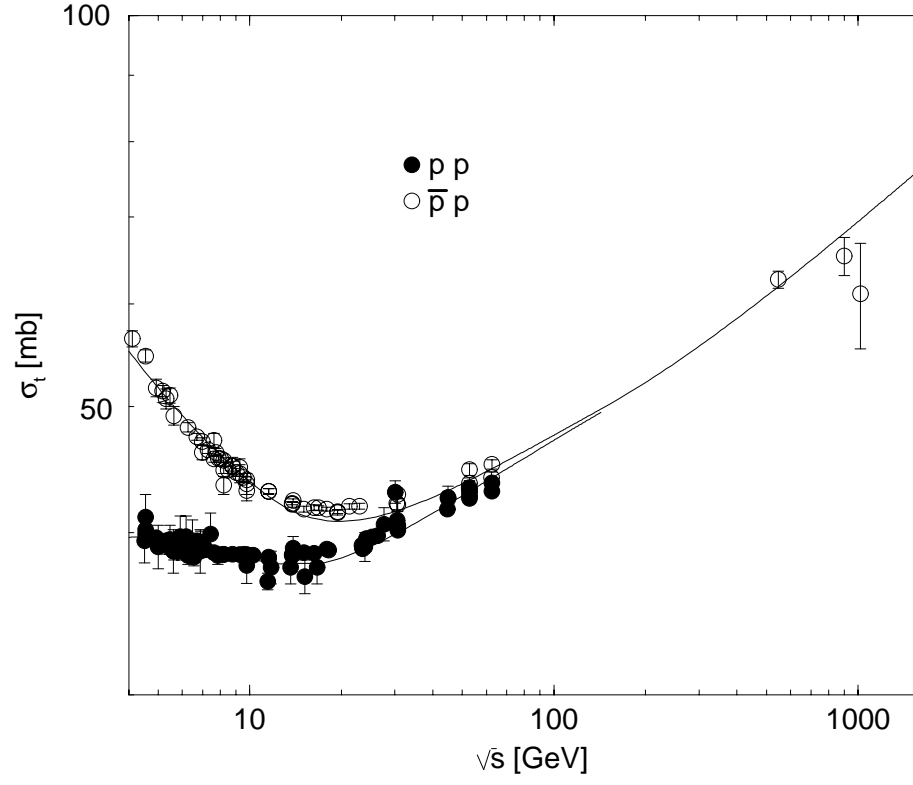


Figure 2: Total cross section calculated up to two gluon rungs and fitted to the $p\bar{p}$ and pp data.

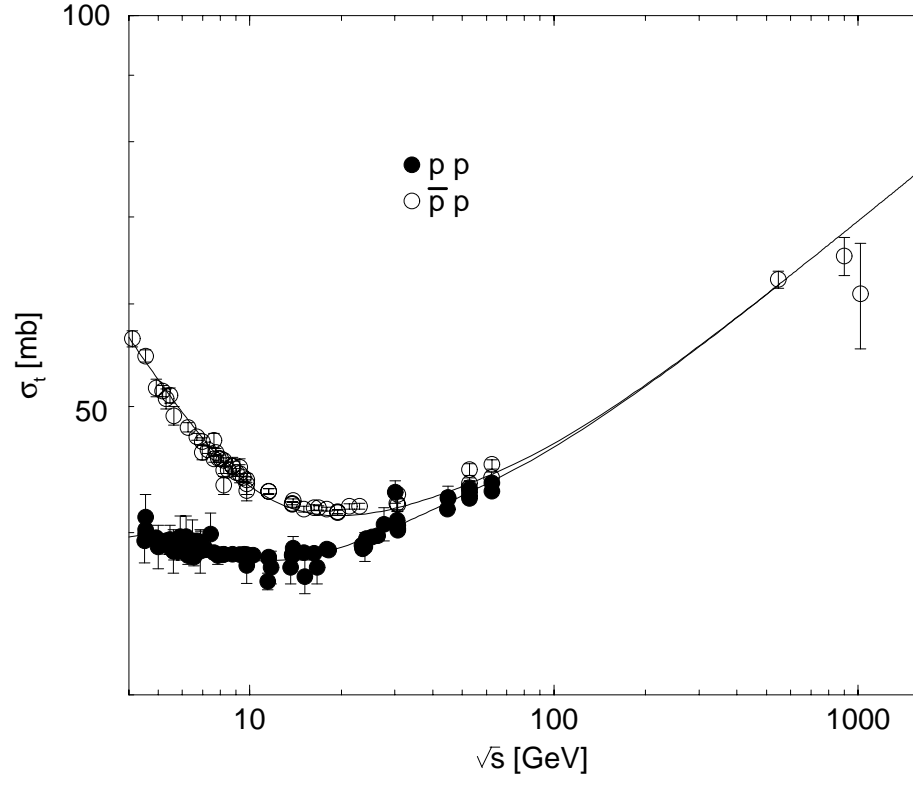


Figure 3: Total cross section calculated up to three gluon rungs and fitted to the $p\bar{p}$ and pp data.